

# $^{12}\text{O}$ resonant structure evaluated by two-proton emission process

T. N. Leite<sup>1</sup>, N. Teruya<sup>2</sup>, A. Dimarco<sup>3</sup>, S. B. Duarte<sup>4</sup>, O. A. P. Tavares<sup>4</sup> and M. Gonçalves<sup>5</sup>

<sup>1</sup> Colegiado de Engenharia Civil,  
Fundação Universidade Federal do Vale do São Francisco - UNIVASF,  
C. Postal 309, 48900-000, Juazeiro - BA, Brazil;

<sup>2</sup> Departamento de Física, Universidade Federal da Paraíba - UFPB,  
Campus de João Pessoa, C. Postal 5008, 58051-970, João Pessoa - PB, Brazil;

<sup>3</sup> Departamento de Ciências Exatas e Tecnológicas - DCET,  
Universidade Estadual de Santa Cruz - UESC,  
Rodovia Ilhéus - Itabuna Km 16, 45650-000, Ilhéus - BA, Brazil;

<sup>4</sup> Centro Brasileiro de Pesquisas Físicas - CBPF/MCT,  
Rua Dr. Xavier Sigaud 150, 22290-180, Rio de Janeiro - RJ, Brazil;

<sup>5</sup> Instituto de Radioproteção e Dosimetria - IRD/CNEN,  
Av. Salvador Allende s/n, 22780-160, Rio de Janeiro, RJ, Brazil.

June, 2009

The characteristics of  $^{12}\text{O}$  resonant ground state are investigated through the analysis of the experimental data for the two-proton decay process. The sequential and simultaneous two-proton emission decay modes have been considered in a statistical calculation of the decay energy distribution. The resonant structures of  $^{11}\text{N}$  have been employed as intermediate states for the sequential mode, having their parameters determined by considering the structure of single particle resonance in quantum scattering problem. The width of  $^{12}\text{O}$  resonant ground state has been extracted from a best fit to the experimental data. The contributions from the different channels to the decay energy distribution have been evaluated, and width and peak location parameters of  $^{12}\text{O}$  resonant ground state are compared with results of other works for the sequential and simultaneous two-proton decay modes.

Pacs: 21.10.-k, 21.10.Pc, 21.60.Gx, 23.50.+z.

## I. INTRODUCTION

The particle radioactivity in nuclei far away from the  $\beta$ -stability line has been presented as an important subject in nuclear physics research. Recently, a large number of publications has been reported on proton radioactivity, both for cases of one proton emission [1–6] and two-proton decay mode [7–12]. A very stimulating discussion concerning the competing mechanisms for the two-proton decay process has gained special attention, since data for two-proton emission are still scarce and not sufficiently elucidative for the contribution of the double sequential single-proton decay mode and of two-proton simultaneous emission of the process. In the sequential mode, after the first proton emission, an intermediate residual nucleus is left in an excited state in continuum, from which the second proton is emitted. This situation is favored by decaying systems populating an intermediate residual nuclear state, which is also a one proton emitter nucleus.

More recently, new experimental data [7] have indicated events related to two-proton emission from  $^{54}\text{Zn}$ . This nucleus, and two other ones ( $^{45}\text{Fe}$  and  $^{48}\text{Ni}$ ) constitutes a set of nuclei very close to the proton drip line, doubly or almost-doubly magic nuclei, which may decay either through emission of a  $^2\text{He}$  system [13], or a three-body simultaneous two-proton emission mechanism[14]. For these two-proton emitter nuclei at the  $A \sim 50$  mass number region there are strong evidences in favor of the simultaneous two-proton emission mode, and these nuclei are not allowed to decay by sequential emission of two protons [15]. On the other hand, the two-proton decay mechanism of  $^{12}\text{O}$  is still not well clarified, persisting a great discussion about the competition between simultaneous and sequential decaying mechanisms. When considering the sequential mode, in general it is supposed that the intermediate proton-emitter  $^{11}\text{N}$  nucleus is populated. The data for  $^{12}\text{O}$  decay energy distribution present a clear peak at  $E_{peak}^{(exp)} \approx 1.77$  MeV [8, 10], however calculations to partial width of the sequential decay are still not well defined, ranging from  $\sim 5$  keV to  $\sim 600$  keV [8–10]. For instance, in Ref.[8] the authors evaluated a width of 578 keV for two-proton emission with the dominance of the sequential decay channel, presenting an upper limit for  $^2\text{He}$  branching ratio to about 7%. On the other hand, the calculation using the three-body theory [12], for sequential and simultaneous mechanisms, provides a smaller width of 66 keV. However, experimental data of Ref.[9] indicate a width of 400 keV which is compatible with a broad diproton branching ratio of 30 – 90 %. These are some experimental evidences favoring the sequential two-proton emission from  $^{12}\text{O}$  nucleus. An important point to determine the contribution from the different decaying processes is the

knowledge of the intermediate nuclear structures involved in the proton emission process.

In the present work we have obtained the width and peak location of the  $^{12}\text{O}$  resonant ground state by considering both decay modes, the sequential and the simultaneous two-proton emission. The lowest energy single-proton resonant structure of  $^{11}\text{N}$  is taken as intermediate state to describe the sequential decay mode. The treatment of the simultaneous emission channel includes the two modes of direct proton pair emission from  $^{12}\text{O}$  resonant ground state, i.e., the one with the emission of a strong correlated pair, the diproton emission, and the case for two-proton decay leaving the three-body final state to the system. It is important to note that the decay energy spectrum does not seem to distinguish these two situations, whereas the decay angular distribution (as pointed out in Fig. 3 of Ref [8]) shows distinct behavior for these different modes.

Besides the width and peak location of  $^{12}\text{O}$  resonant ground state we also determine the contributions from the sequential and simultaneous decay channels at each decay energy value. Finally, our results are compared with partial widths of different decay channels obtained in other works.

## II. CHANNELS DESCRIPTION AND THEIR INTERMEDIATE STATES

The ground-state of  $^{12}\text{O}$  nucleus is evaluated in connection with previous calculations [3] for low-lying states of the proton emitter nucleus  $^{11}\text{N}$ , which are taken as intermediated states of the sequential decay mode. The single-particle resonant states of  $^{11}\text{N}$  are determined for a system composed of a single-proton orbiting the  $^{10}\text{C}$  core. The proton state is described by a resonant state of the system  $^{10}\text{C}+1\text{p}$  in the continuum. The main contribution of the continuum to resonant state structure is accounted for by using the discrete levels with the complex energies approximation. This is a so-called continuum projection method [3, 16] in which the quantum scattering problem is treated by using orthogonal and complementary projectors to write the scattering wave function as  $|\psi^+\rangle = |u\rangle\langle u|\psi^+\rangle + P|\psi^+\rangle$ , where  $|u\rangle$  is a normalized single-particle state and  $P = 1 - |u\rangle\langle u|$  projects onto the complementary subspace of the single particle Hilbert space. Therefore, projection and formal manipulation of the Schrödinger equation,  $(E - H)|\psi^+\rangle = 0$ , rises the nonhomogeneous equation,

$$(E - H)|\varphi^+\rangle = \alpha|u\rangle,$$

where  $|\varphi^+\rangle$  is the scattering solution of the projected Hamiltonian  $H_{pp}$  ( $\equiv P H P$ ) at energy  $E$ . The normalized single-particle state  $|u\rangle$  is chosen proportional to the internal part of

TABLE I: The two lowest single-particle resonant states calculated in Ref. [3] for the unbound  $^{11}\text{N}$  nucleus are presented in comparison with recent experimental data [4, 5].

$j^\pi$	our previous results		experimental data			
	Ref. [3]		Ref. [4]		Ref. [5]	
	$E_j(\text{MeV})$	$\Gamma_j(\text{MeV})$	$E_j(\text{MeV})$	$\Gamma_j(\text{MeV})$	$E_j(\text{MeV})$	$\Gamma_j(\text{MeV})$
$\frac{1}{2}^+$	1.38	0.59	1.27	1.44	1.54	0.83
$\frac{1}{2}^-$	2.18	0.51	2.01	0.84	2.27	1.15
$\frac{5}{2}^+$	3.77	0.47	3.75	0.60	3.61(5)	0.50(8)
$\frac{3}{2}^+$	4.81	0.86	4.50	1.27	—	—

the resonant wave function  $|\psi^+\rangle_{E=\varepsilon_0}$ , which is the solution of the homogeneous equation at the energy  $\varepsilon_0$ . The  $\varepsilon_0$  value is defined as the energy where the integral of the internal part of the density of probability is maximum. The complex single-particle energy,

$$\varepsilon_u - \frac{i\Gamma_u}{2} = \langle u|H|u\rangle + \langle u|H(E + i\eta - H_{pp})^{-1}H|u\rangle, \quad (1)$$

is calculated at  $\varepsilon_0$ ;  $\varepsilon_u$  gives the position of the resonant peak and  $\Gamma_u$  corresponds to its width. The coefficient  $\alpha = -\langle u|H|\varphi^+\rangle$  is adjusted to satisfy the orthogonal condition  $\langle u|\varphi^+\rangle = 0$ , therefore resulting the width,

$$\Gamma_u = 2\pi |\alpha|^2. \quad (2)$$

The calculation has been performed by using a single-particle Hamiltonian composed of a spherical Woods-Saxon potential, a spin-orbit term with a Woods-Saxon derivative form, a centrifugal barrier, and the Coulomb term for a uniformly charged sphere. The  $^{12}\text{O}$  sequential proton emission mode can occur through different channels involving an intermediate state of  $^{11}\text{N}$  having total angular momentum  $j$ , namely,



The one-proton decay width for the considered  $^{11}\text{N}$  intermediate resonant states were previously calculated [3] (values in Table-I). The use of  $^{10}\text{C}$  nucleus as an inert core to the calculation of  $^{12}\text{O}$  and  $^{11}\text{N}$  structures can be supported by relevant data regarding  $^{10}\text{C}$  nuclear properties: i) its ground state has a half-life of 19.2 s, and spin and parity  $J^\pi = 0^+$ ; ii) the neutron and proton separation energies,  $S_{1n} = 21.3$  MeV,  $S_{1p} = 4.0$  MeV,  $S_{2p} = 3.8$  MeV and  $S_{2n} = 35.5$  MeV [17] are all greater than those relevant for  $^{11}\text{N}$  and  $^{12}\text{O}$  nuclei.

As mentioned before, the simultaneous direct emission mode can occur by the so called diproton emission or by generating a three body final state. However, regarding the determination of the decay energy spectrum, these two situations can be considered together, as a single simultaneous emission channel, since these decay modes do not involve any intermediate nuclear state. In both cases the two protons are emitted in a single step of the decay process from the same original nuclear resonant structure, the  $^{12}\text{O}$  ground state.

### III. $^{12}\text{O}$ RESONANT GROUND STATE EVALUATION

In order to determine the characteristic parameter-values for  $^{12}\text{O}$  resonant state we have introduced a phenomenological procedure to describe the existing data for the decay energy spectrum obtained by measuring in-coincidence the two proton kinetic energies. The method is based on a statistical analysis of the events generated along the decay process. Firstly, we consider the events generated in the sequential channels, connecting the measured values of proton energies with the energy distribution of the resonant states involved in the process. For instance, in the sequential channels,



the probability density of having  $^{12}\text{O}$  resonant state decaying around a given energy-value  $E$  in the first step of the process is given by,

$$\frac{dP_0}{dE} \sim \frac{\Gamma_0}{(E - E_0)^2 + (\Gamma_0/2)^2}. \quad (4)$$

The amount of energy  $E$  should be partitioned between the first emitted proton kinetic energy  $\varepsilon_1$  and the energy  $\varepsilon_2$  left to the  $^{11}\text{N}$  resonance intermediated state,  $E = \varepsilon_1 + \varepsilon_2$ . Consequently we can label each partition configuration of the energy  $E$  by the value  $\varepsilon_2$ , corresponding to the energy carried out by the second proton in the last step of the process. Since this proton is emitted from the  $j^{\text{th}}$  intermediate resonant state the probability associated to the occurrence of **any** partitions of the energy  $E$  is given by

$$P_j(E) \sim \frac{\Gamma_j}{\sum_j \Gamma_j} \int_0^E d\varepsilon_2 \frac{\Gamma_j}{(\varepsilon_2 - E_j)^2 + (\Gamma_j/2)^2}. \quad (5)$$

The branching factor of the  $j^{\text{th}}$ - channel in the above expression takes into account the probability of incidence of this channel among the other sequential ones. Alternatively, this

is the probability of having the proton emitted from the resonance in the  $j^{\text{th}}$  – channel with any energy value  $\varepsilon_2 < E$  . So, the probability density of detecting a decay event in  $j^{\text{th}}$  channel with proton-pair energy around  $E$  can be written as

$$\frac{dS_j}{dE} \sim \frac{\Gamma_0}{(E - E_0)^2 + (\Gamma_0/2)^2} \times \frac{\Gamma_j}{\sum_j \Gamma_j} \left[ \int_0^E d\varepsilon_2 \frac{\Gamma_j}{(\varepsilon_2 - E_j)^2 + (\Gamma_j/2)^2} \right], \quad (6)$$

with these distributions easily normalized in the interval  $[0, \infty]$ .

In this statistical analysis the description of the simultaneous emission can be thought as a limit of the previous sequential case as the time interval between the steps goes to zero, and using the same decaying initial resonant structure as a *pseudo-intermediate* state. According to this assumption the simultaneous channel decay energy distribution is obtained directly from Eq.(6) by taking for the resonant state parameters in Eq.(5) the values  $\Gamma_j = \Gamma_0$  and  $E_j = E_0$ , leading to

$$\frac{dS_0}{dE} \sim \frac{\Gamma_0}{(E - E_0)^2 + (\Gamma_0/2)^2} \times \frac{\Gamma_0}{\sum_j \Gamma_j} \int_0^E d\varepsilon_2 \frac{\Gamma_0}{(\varepsilon_2 - E_0)^2 + (\Gamma_0/2)^2}, \quad (7)$$

Now, Eq.(6) can be considered valid also to the simultaneous channel, with the  $j$ –index covering the values  $j = 0 ; \frac{1}{2}^- ; \frac{1}{2}^+ ; \frac{5}{2}^+ ; \frac{3}{2}^+$  . By performing analytically the integrals in Eqs(6 and (7), the decay energy distribution through  $j^{\text{th}}$  channel reads,

$$\frac{dS_j}{dE} \sim \frac{\Gamma_0}{(E - E_0)^2 + (\Gamma_0/2)^2} \times \frac{\Gamma_j}{\sum_j \Gamma_j} \left( \tan^{-1} \frac{E - E_j}{\Gamma_j/2} + \tan^{-1} \frac{E_j}{\Gamma_j/2} \right). \quad (8)$$

We remark that there are only two unknown parameters,  $E_0$  and  $\Gamma_0$  in the expressions for the channel energy distributions in Eqs.(6-8). These parameter-values were determined by the  $\chi$ -square value minimization of the total energy distribution,

$$\frac{dS}{dE} = \sum_j \frac{dS_j}{dE}, \quad (9)$$

to the experimental data by Kryger et al [8] in the region of the largest peak. For this adjustment we have a final normalization of the  $dS/dE$  distribution to the experimental peak value, and we have used the set of values  $\{(\Gamma_j; E_j), j \neq 0\}$  in the first column of Table-I as in Ref. [3]. These values were previously determined by applying the method in Section I to obtain the one-body resonant states of the  $^{11}\text{N}$  listed in Table-I for  $j = \frac{1}{2}^- ; \frac{1}{2}^+ ; \frac{5}{2}^+ ; \frac{3}{2}^+$  . Our preference by the use of a confident theoretical prediction (instead of the existing experimental values) is justified by the purpose of future application of our calculation

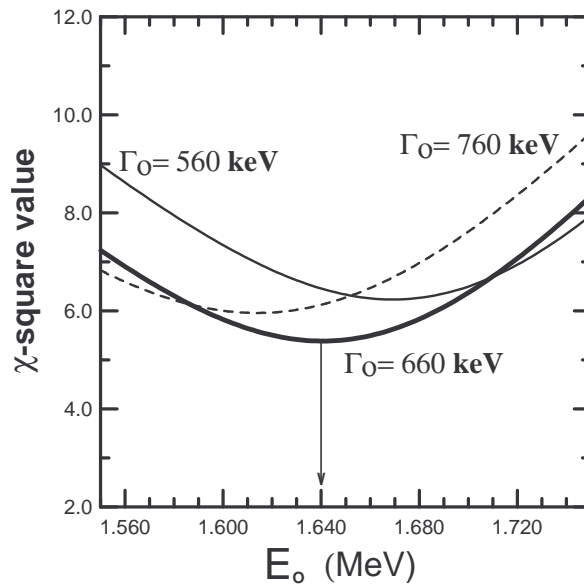


FIG. 1: The  $\chi$ -square values for the determination of  $E_0$  and  $\Gamma_0$  in the adjustment process of  $dS/dE$  energy distribution to the experimental data.

to other two-proton emission cases, in which the characteristics of the adopted nuclear intermediate states are not measured yet.

Our best result of the fit for experimental data by Kryger et al [8] has been obtained as  $E_0 = 1640$  keV and  $\Gamma_0 = 660$  keV. In Fig.1 we illustrate the changes of  $\chi$ -square values around its minimum by varying of  $E_0$  and  $\Gamma_0$  parameter-values. The best result for the total energy distribution adjustment is displayed in Fig.2 (full line), also showing the experimental data of Ref. [8] (points with error bars). In addition, we can define the fractional  $j$ -channel contribution for a given decay energy value along the spectrum,

$$R_j(E) = \frac{dS_j/dE}{dS/dE}. \quad (10)$$

This quantity is shown in Fig.3, where one can see that the simultaneous decay curve (dashed curve) presents values similar to that ones of the sequential channels curves for  $j = \frac{1}{2}^+$ . However, the outgoing channel branching can be calculated after the determination of the  $E_0$  and  $\Gamma_0$ , with the best adjusted distribution

$$B_j = \frac{\int_0^\infty dE (dS_j/dE)}{\int_0^\infty dE (dS/dE)}. \quad (11)$$

The founded values are,

$$B_0 = 37 \% \quad ; \quad B_{\frac{1}{2}^+} = 42 \% \quad ; \quad B_{\frac{1}{2}^-} = 14 \% \quad ; \quad B_{\frac{5}{2}^+} = 3 \% \quad ; \quad B_{\frac{3}{2}^+} = 4 \% \quad .$$

Table-II shows results from other works for the different modes of  $^{12}\text{O}$  two-proton emission process. Note that in the case of  $^{12}\text{O}$  two-proton emission process there are some different sets of data for the parameters of the intermediate states (see Table-I), so it is important to repeat the calculation for  $^{12}\text{O}$  decay spectra by using directly the  $^{11}\text{N}$  experimental data. With this procedure we are also verifying the sensibility of our approach in respect to the variation of the  $^{11}\text{N}$  parameters. We replicate the calculation by using the  $^{11}\text{N}$  experimental result of Ref. [4], and the best  $\chi$ -square adjustment gave the values  $E_0 = 1660$  keV and  $\Gamma_0 = 640$  keV, which are comparable to the obtained previously (see Fig.1). The decay spectra obtained from these values are represented by the dashed line in Fig. 2, and their respective branching values  $B_j$ 's are,

$$B_0 = 22 \% \ ; \ B_{\frac{1}{2}^+} = 51 \% \ ; \ B_{\frac{1}{2}^-} = 19 \% \ ; \ B_{\frac{5}{2}^+} = 3 \% \ ; \ B_{\frac{3}{2}^+} = 5 \% \ .$$

In Ref-[8] the analysis of experimental data by using the R-matrix formalism is compatible with a dominance of the sequential emission mode for the two-proton energy spectrum, with a width of  $\simeq 580$  keV. On the other side, the branching ratio for the diproton emission had an upper limit of 7%. Another R-matrix calculation for diproton emission, performed in Ref. [9], offers an upper limit of 5 keV for this width, while the width for sequential decay must be less than 100 keV.

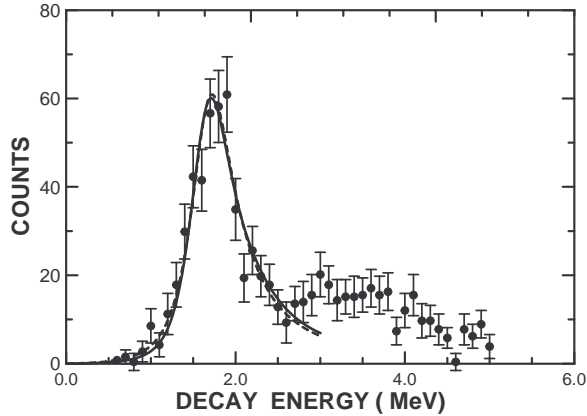


FIG. 2: Decay-energy distribution for the structure of  $^{12}\text{O}$  resonant ground-state. The full line is the result obtained by using theoretical predictions for  $^{11}\text{N}$  parameters in Table-I. The dashed line is the result obtained by using the experimental data for  $^{11}\text{N}$  intermediate state parameters in Ref. [4]. Points are the experimental spectra by Kryger et al [8], with the experimental peak-value being used in the normalization of our results.



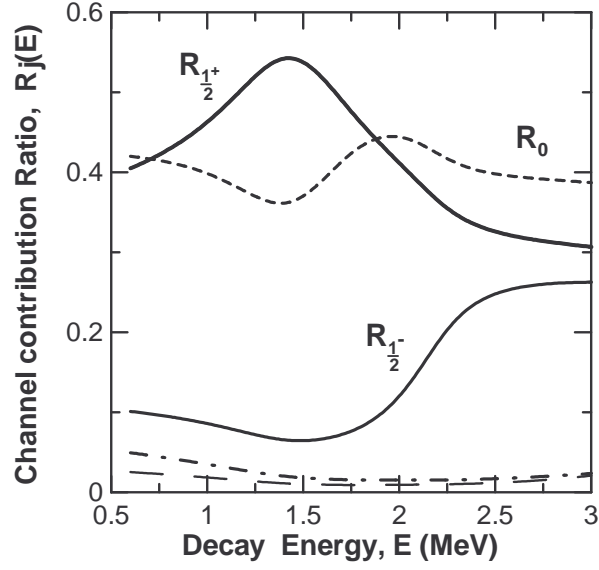


FIG. 3: Channel contributions  $R_j(E)$  to the decay energy spectrum as defined in Eq.(10). The dash-dotted curve is for  $j = \frac{5}{2}^+$ , and the long dashed one corresponds to the smallest contribution for  $j = \frac{3}{2}^+$ . The other curves are specified by the corresponding label. Results have been obtained by using theoretical predictions for  $^{11}\text{N}$  parameters in Table-I.

TABLE II: Recent experimental and theoretical results for resonant  $^{12}\text{O}$  ground-state.

Reference	$E_{peak}$ (MeV)	Decay width $\Gamma$ (keV)	
		diproton decay	Sequential emission
		$\Gamma_{2p}$	$\Gamma_{p-p}$
Kryger <i>et al.</i> [8]	1.77	–	578
Kekelis <i>et al.</i> [10]	1.82	400	–
Sherr and Fortune [11]	1.78	340	–
Barker [9]	1.78	< 5	< 100
Grigorenko[12]			60 – 100

#### IV. SUMMARY AND CONCLUSION

In short, we have determined the  $^{12}\text{O}$  resonant ground state characteristics, and to accomplish the calculation, we have determined the two proton energy distribution in terms of  $^{11}\text{N}$  parameters of resonant intermediate states.

The introduced phenomenological method in section III is a calculation procedure based in statistical concepts, permitting to constructed expression to the total energy distribution (Eq.9). From the adjustment of this distribution to experimental data we obtained the unknown parameter values of the  $^{12}\text{O}$  resonant ground. Results to best adjusted of the total energy distribution and for the channel contributions are displayed in Fig.2 and Fig.3, respectively. In Table-II we compared our results for the sequential emission and diproton decay widths with that ones from other works [8, 9].

We recall that in spite of the invariant mass spectrum data still show some concerning to the experimental peak width value, the method of analysis here introduced is a useful and efficient tool to extract information about  $^{12}\text{O}$  ground state. We are showing that if we have by hand a well determined experimental decay energy spectrum the characteristics of the resonant emitter ground state nuclide can be obtained with satisfactory accuracy by the using present statistical analysis in section III.

As a final point, we call attention to the fact that the phenomenological procedure to determine  $^{12}\text{O}$  resonant ground-state characteristics reported here may also be applied to any other two-proton emitter nuclide with high contribution from the continuum state in their spectrum, provided that the experimental data for the two-proton decay energy distribution and parameters of intermediate nuclear resonant states are known.

#### Acknowledgements

One of the authors (SBD) thanks to the Brazilian CNPq for partial financial support.

- 
- [1] S. Aberg, P. B. Semmes and W. Nazarewicz, Phys. Rev. **C 56**, 1762 (1997).
  - [2] C. N. Davids and H. Esbensen, Phys. Rev. **C 61**, 054302 (2000).
  - [3] T. N. Leite, N. Teruya and H. Dias, Int. J. Mod. Phys. **E 11**, 469 (2002).
  - [4] K. Markenroth *et al*, Phys. Rev. **C 62**, 034308 (2000).

- [5] E. Casarejos *et al*, Phys. Rev. **C 73**, 014319 (2006).
- [6] E. L. Medeiros, M. M. N. Rodrigues, S. B. Duarte, and O. A. P. Tavares, Eur. Phys. J **A 34**, 417 (2007).
- [7] B. Blank *et al*, Phys. Rev. Lett. **94**, 232501 (2005).
- [8] R. A. Kryger *et al*, Phys. Rev. Lett. **74**, 860 (1995); A. Azhari, R. A. Kryger, and M. Thoennessen, Phys. Rev. **C 58**, 2568 (1998).
- [9] F. C. Barker, Phys. Rev. **C 59**, 535 (1999); **63**, 047303 (2001).
- [10] G. J. KeKelis *et al*, Phys. Rev. **C 17**, 1929 (1978).
- [11] R. Sherr, and H. T. Fortune, Phys. Rev. **C 60**, 064323 (1999).
- [12] L. V. Grigorenko, I. G. Mukha, I. J. Thompson and M. V. Zhukov, Phys. Rev. Lett. **88**, 042502 (2002).
- [13] B. Blank *et al*, Phys. Rev. Lett. **84**, 1116 (2000).
- [14] K. Miernik *et al*, Phys. Rev. Lett. **99**, 192501 (2007).
- [15] J. Giovinazzo *et al*, Phys. Rev. Lett. **99**, 102501 (2007).
- [16] N. Teruya, H. Dias and A. F. R. de Toledo Piza, Nucl. Phys. **A 556**, 157 (1993).
- [17] G. Audi, A. H. Wapstra and C. Thibault, Nucl. Phys. **A729**, 337 (2003).